JACC: CARDIOVASCULAR IMAGING VOL. 8, NO. 10, 2015

ISSN 1936-878X/$36.00
PUBLISHED BY ELSEVIER INC. http://dx.doi.org/10.1016/j.jcmg.2015.04.024

Coronary Artery Axial Plaque Stress and its Relationship With Lesion Geometry

Application of Computational Fluid Dynamics to Coronary CT Angiography

Gilwoo Choi, PhD,*† Joo Myung Lee, MD, MPH,‡ Hyun-Jin Kim, PhD,* Jun-Bean Park, MD,‡ Sethuraman Sankaran, PhD,* Hiromasa Otake, MD, PhD,§ Joon-Hyung Doh, MD, PhD,‖ Chang-Wook Nam, MD, PhD,¶ Eun-Seok Shin, MD, PhD,# Charles A. Taylor, PhD,** Bon-Kwon Koo, MD, PhD†††

ABSTRACT

OBJECTIVES The purpose of this study was to characterize the hemodynamic force acting on plaque and to investigate its relationship with lesion geometry.

BACKGROUND Coronary plaque rupture occurs when plaque stress exceeds plaque strength.

METHODS Computational fluid dynamics was applied to 114 lesions (81 patients) from coronary computed tomography angiography. The axial plaque stress (APS) was computed by extracting the axial component of hemodynamic stress acting on stenotic lesions, and the axial lesion asymmetry was assessed by the luminal radius change over length (radius gradient [RG]). Lesions were divided into upstream-dominant (upstream RG > downstream RG) and downstream-dominant lesions (upstream RG < downstream RG) according to the RG.

RESULTS Thirty-three lesions (28.9%) showed net retrograde axial plaque force. Upstream APS linearly increased as lesion severity increased, whereas downstream APS exhibited a concave function for lesion severity. There was a negative correlation ($r = -0.274$, $p = 0.003$) between APS and lesion length. The pressure gradient, computed tomography–derived fractional flow reserve (FFR_{CT}), and wall shear stress were consistently higher in upstream segments, regardless of the lesion asymmetry. However, APS was higher in the upstream segment of upstream-dominant lesions ($11{,}371.96 \pm 5{,}575.14$ dyne/cm^2 vs. $6{,}878.14 \pm 4{,}319.51$ dyne/cm^2, $p < 0.001$), and in the downstream segment of downstream-dominant lesions ($7{,}681.12 \pm 4{,}556.99$ dyne/cm^2 vs. $11{,}990.55 \pm 5{,}556.64$ dyne/cm^2, $p < 0.001$). Although there were no differences in FFR_{CT}, % diameter stenosis, and wall shear stress pattern, the distribution of APS was different between upstream- and downstream-dominant lesions.

CONCLUSIONS APS uniquely characterizes the stenotic segment and has a strong relationship with lesion geometry. Clinical application of these hemodynamic and geometric indices may be helpful to assess the future risk of plaque rupture and to determine treatment strategy for patients with coronary artery disease. (Evaluation of FFR, WSS, and TPF Using CCTA; NCT01857687) (J Am Coll Cardiol Img 2015;8:1156–66)

From *HeartFlow, Redwood City, California; †Department of Surgery, Stanford University Medical Center, Stanford, California; ‡Department of Medicine, Seoul National University Hospital, Seoul, South Korea; §Department of Medicine, Kobe University Graduate School of Medicine, Kobe, Japan; ‖Department of Medicine, Inje University Ilsan Paik Hospital, Goyang, South Korea; ¶Department of Medicine, Keimyung University Dongsan Medical Center, Daegu, South Korea; #Department of Cardiology, Ulsan University Hospital, University of Ulsan College of Medicine, Ulsan, South Korea; **Department of Bioengineering, Stanford University, Stanford, California; and the ††Institute on Aging, Seoul National University, Seoul, South Korea. This study was funded by HeartFlow. Drs. Choi, Kim, Sankaran, and Taylor are employees and shareholders of HeartFlow, which provided the FFR_{CT} service. Dr. Koo has received an institutional research grant from St. Jude Medical. All other authors have reported that they have no relationships relevant to the contents of this paper to disclose. The first 2 authors contributed equally to this work.

Manuscript received January 12, 2015; revised manuscript received March 24, 2015, accepted April 2, 2015.

Coronary plaque rupture is a critical event that triggers the initiation of acute coronary syndrome (ACS). Although the sequence of plaque rupture is well understood with previously reported histopathological data (1), the prediction of plaque rupture in an individual patient is still problematic. To assess the risk of ACS, image-based findings such as cap thickness, presence of a lipid core, and the degree of inflammation have been proposed as the key features of vulnerable plaques (2). However, plaque rupture can occur whenever plaque stress exceeds the plaque strength in a similar mechanism to general mechanical material failures (3,4). Therefore, if the imbalance between plaque durability and external force can be assessed simultaneously, prediction of the risk of plaque rupture can be more accurate.

SEE PAGE 1167

Among various hemodynamic forces, wall shear stress (WSS) has been proposed as a key hemodynamic force affecting the initiation, progression, and transformation of atherosclerotic plaque from a stable to unstable phenotype (1,3,5,6). However, the magnitude of WSS is significantly smaller than other components of hemodynamic forces such as pressure, and thus WSS alone may not act as a direct force for the occurrence of plaque rupture. The coronary arteries are under circumferential and axial tension resulting from blood pressure. A net anterograde axial force on the plaque (largely due to the pressure gradient) would increase the axial tension and plaque stress on the upstream segment of the plaque but decrease those acting on the downstream end of the plaque. The converse is true for a net retrograde axial force on the plaque, which, paradoxically, can occur for certain plaque geometries despite the minimal pressure gradient acting on the downstream segment of a plaque. These net axial forces may explain the clinical observation that plaque rupture occurs on both upstream and downstream segments of a plaque (7,8).

Recent advances in coronary computed tomography angiography (CTA) and computational fluid dynamics (CFD) technologies enable quantification of hemodynamic forces acting on plaques with more accurate patient-specific geometric models and physiological boundary conditions than have been possible heretofore (9).

The purpose of this study was to characterize the hemodynamic forces acting on coronary plaques and to investigate its relationship with lesion geometry using CFD applied to coronary models created from coronary CTA data of patients with coronary artery disease.

METHODS

Plaque force analysis for human coronary lesions was performed to investigate hemodynamic forces in real patient data and then idealized stenosis models were analyzed to confirm the findings from patient data. Detailed description of the idealized model study is presented in the Online Appendix.

PATIENT POPULATION. A total of 81 patients presenting with stable angina and suspected coronary artery disease were included for this study from 4 cardiovascular centers in Korea and Japan (**Table 1**). The inclusion criteria were patients with stable angina, the existence of coronary CTA, invasive coronary angiography, and fractional flow reserve (FFR) measurement within an interval of <3 months between coronary CTA and invasive procedures. The study protocol was approved by the institutional review boards of each site, and was in accordance with the Declaration of Helsinki (NCT01857687).

INVASIVE CORONARY ANGIOGRAPHY AND INVASIVE FFR. Selective invasive coronary angiography was performed by standard techniques. All angiograms were reviewed at a core laboratory in a blinded fashion. The FFR was measured using a 0.014-inch pressure-monitoring guidewire (St. Jude Medical, Uppsala, Sweden) in vessels with coronary artery disease. Maximal hyperemia was induced with a continuous intravenous infusion of adenosine or ATP at the rate of 140 μg/kg/min.

IMAGE ACQUISITION OF CORONARY CTA. The coronary CTA images were obtained in accordance with the Society of Cardiovascular Computed Tomography Guidelines on performance of coronary CTA, with 64 or higher detector row scanner platforms (10). Oral beta-blockers were administered for any subjects with a heart rate ≥65 beats/min. Immediately before the coronary CTA acquisition, 0.2 mg of sublingual nitroglycerin was administered.

CFD ANALYSIS OF THE LESION IN PATIENTS WITH CORONARY ARTERY DISEASE. Coronary models constructed from coronary CTA were discretized into volumetric meshes for CFD analysis. The boundary conditions of CFD domain were assigned on the basis of vessel sizes at each outlet, assuming a hyperemic condition as described by Taylor et al. (9). Briefly, the basal outlet resistances at rest were determined from the fundamental form-function relationships relating organ flow with organ size according to metabolic demands. Specifically, an allometric scaling law was used to estimate the total coronary flow based on

ABBREVIATIONS AND ACRONYMS

ACS = acute coronary syndrome

APS = axial plaque stress

CFD = computational fluid dynamics

CTA = computed tomography angiography

FFR = fractional flow reserve

FFR_{CT} = coronary computed tomography angiography-derived fractional flow reserve

MLA = minimal lumen area

RG = radius gradient

WSS = wall shear stress

TABLE 1 Baseline Characteristics of the Patients

Patients (N = 81)	
Age, yrs	63.8 ± 9.0
Female	12 (15.0)
Body mass index, kg/m^2	24.5 ± 2.1
Median interval between coronary CTA and ICA, days	29
Lesion characteristics (N = 114)	
Lesion location	
Left main to LAD	72 (64.0)
LCX	19 (16.7)
RCA	22 (19.3)
Coronary CTA	
MLA, mm^2	2.04 ± 0.94
% area stenosis	61.98 ± 13.14
Distance from coronary ostium to MLA, mm	40.39 ± 16.77
Lesion length, mm	14.25 ± 5.52
FFR_{CT}	0.78 ± 0.12
Invasive FFR	0.79 ± 0.11

Values are mean ± SD or n (%).

CTA = computed tomography angiography; FFR_{CT} = coronary computed tomography angiography-derived fractional flow reserve; FFR = fractional flow reserve; ICA = invasive coronary angiography; LAD = left anterior descending coronary artery; LCX = left circumflex coronary artery; MLA = minimal lumen area; RCA = right coronary artery.

myocardial mass, and a morphometry law was used to relate the resistance of the microcirculation downstream of a vessel to the vessel size at each outlet. The outlet resistance was then reduced by utilizing a mathematical model of hyperemic condition derived from the effect of adenosine on reducing the resistance of the coronary microcirculation. Finally, CFD analysis was performed on the discretized model of geometry with boundary conditions, to numerically solve the governing equations of fluid dynamics as a Newtonian fluid. The numerical solutions of flow and pressure fields were then used to compute hemodynamic forces on complete spatial domain of geometry including traction and wall shear stress (9).

Stenotic lesions were determined by a visual angiographic evaluation (>30% stenosis), and corresponding lesions were identified in coronary CTA images. To understand the regional variation of hemodynamic characteristics, each stenotic lesion was subdivided into upstream and downstream segments with respect to the location of minimal lumen area (MLA). Hemodynamic parameters including fractional flow reserve from coronary computed tomography angiography (FFR_{CT}), WSS, pressure, pressure change over length (pressure gradient), traction, and axial plaque force were computed from CFD analysis. All coronary CTA-based geometry constructions and CFD analyses were performed by a single core laboratory, HeartFlow (Redwood City, California).

ANALYSIS OF HEMODYNAMIC FORCES. The internal stress and strain within the plaque would ultimately affect the plaque rupture, but this internal stress and strain is directly related to the external force, that is, a high external force increases the internal stress in the plaque. The total force acting on plaques or luminal surfaces is the traction force. If the traction force is divided by the area on which it acts, the term is then called the traction with units of force per unit area. A typical decomposition of traction is with respect to the normal direction of the luminal surface, resulting in the well-known WSS—the tangential component of traction—and pressure—the normal component of traction.

Because the pressure drop mainly occurs in the direction of the vessel across stenotic lesions, that is, axially, another way to decompose traction is based on the centerline direction of the vessel. This approach of decomposing hemodynamic forces introduces a hemodynamic index: axial plaque stress (APS) (**Figure 1**). The APS can be computed by the projection of traction onto the centerline of the coronary artery as follows:

$$\overrightarrow{APS} = (\vec{t} \cdot \vec{c})\vec{c}$$

where $\vec{t}$ is the traction vector, $\vec{c}$ is the unit tangential vector of centerline ($\| \vec{c} \| = 1$), and $(\vec{t} \cdot \vec{c})$ is the dot product of $\vec{t}$ and $\vec{c}$. The radial component of traction was not analyzed in this study because the axial component is expected to be the more relevant contributing factor of force imbalance than the radial component because the main driving force caused by the pressure gradient is along the vessel length in the axial direction.

APS represents a fluid stress imparted to the surface of the plaque and is the main contributor for the imbalance of force across the lesion. The imbalance of external hemodynamic forces ultimately influences the stress within the plaque, and APS uniquely characterizes the stress acting on the upstream and downstream segments of a plaque (**Figure 1**).

The shape of each upstream and downstream segment in the axial direction would affect the direction and magnitude of the APS. Thus, we devised a geometric descriptor to quantitatively describe the axial changes in the legion geometry: radius gradient (RG). The RG was defined by the radius change over lesion length, where radius change refers to the difference between the lesion starting (or ending) point radius and the radius at the location of MLA, and lesion length is defined by the length from the lesion starting (or ending) point to MLA location (Online Figure 1A). Lesions with steeper radius change in upstream than downstream

FIGURE 1 APS and Other Hemodynamic Parameters

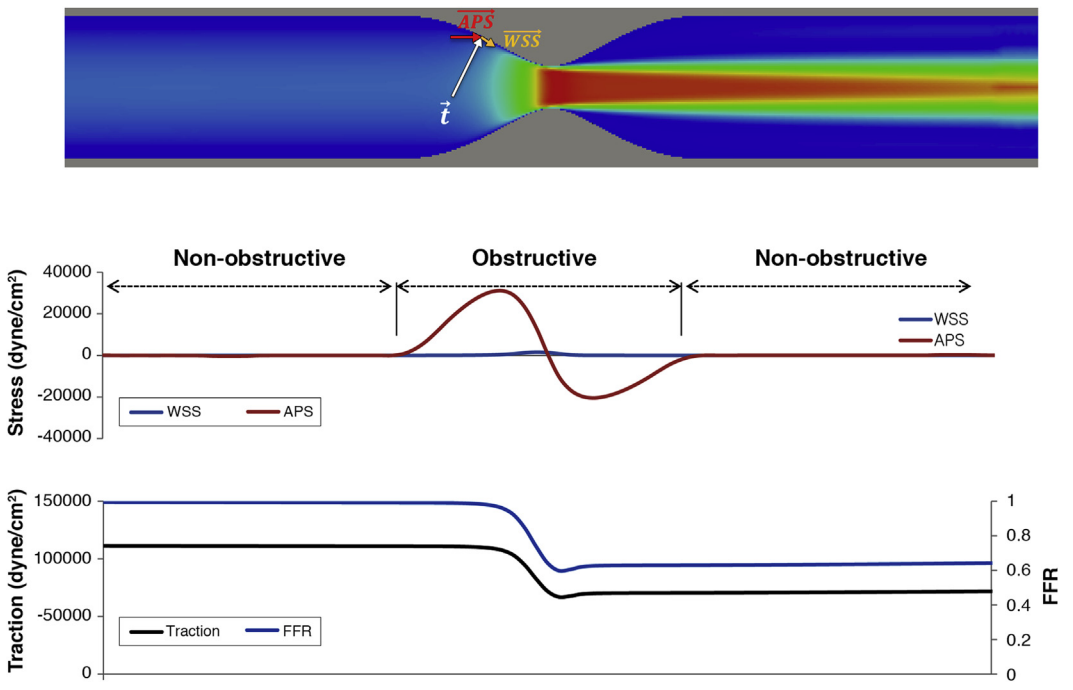

The axial plaque stress (APS) was computed by extracting the axial component of traction acting on the lumen or plaque. Although the magnitudes of traction and FFR decreased along the vessel length, APS uniquely characterized the elevation of hemodynamic stress at upstream and downstream obstructive segments. Note that the magnitude of APS was significantly greater than that of wall shear stress. FFR = fractional flow reserve; WSS = wall shear stress.

(i.e., $RG_{upstream} > RG_{downstream}$) were referred to as "upstream-dominant" lesions, whereas those with steeper radius change in downstream than upstream (i.e., $RG_{downstream} > RG_{upstream}$) were referred to as "downstream-dominant" lesions. To account for local variations in lesion shape, RG was also analytically computed by the average of the radius change over infinitesimal intervals, that is, analytic RG (Online Figure 1B). In patient lesions, those 2 definitions of RG were utilized to investigate its relationship with hemodynamic parameters.

IDEALIZED STENOSIS MODEL. Patient data have diverse clinical presentations, substantial interindividual heterogeneities in the circulatory system, and many unmeasured confounding factors. In order to provide intuitive and simplified explanation of the results from patient lesions, all of the analyses were repeated with an idealized stenosis model. The detailed methods and results from the idealized stenosis model study are presented in the Online Appendix.

STATISTICAL ANALYSIS. Categorical variables were given as counts and percentages; continuous variables were described as mean ± SD, or median and interquartile range as appropriate. Pearson correlation coefficients were calculated to determine the relationship among the hemodynamic parameters pertaining to plaque stress and index of plaque geometry. The comparison of segmental hemodynamic forces between upstream and downstream segments in 1 total plaque was performed with the paired-sample *t* test. For the comparison of hemodynamic forces between upstream-dominant lesions and downstream-dominant lesions, the independent *t*-sample test was used. The interclass correlation coefficient was used to assess the reliability and agreement between the 2 different definitions of RG. All statistical analyses were conducted with SPSS version 18.0 (IBM SPSS Statistics, Chicago, Illinois) and R programming, version 3.0.2 (The R Foundation for Statistical Computing, Vienna, Austria). A 2-sided p value <0.05 was considered as significant.

RESULTS

BASELINE CHARACTERISTICS OF PATIENTS. A total of 81 patients with 114 non-ostial lesions were enrolled (mean age 63.8 ± 9.0 years, male 85.1%). The

FIGURE 2 Distribution of APS in Patients' Lesions

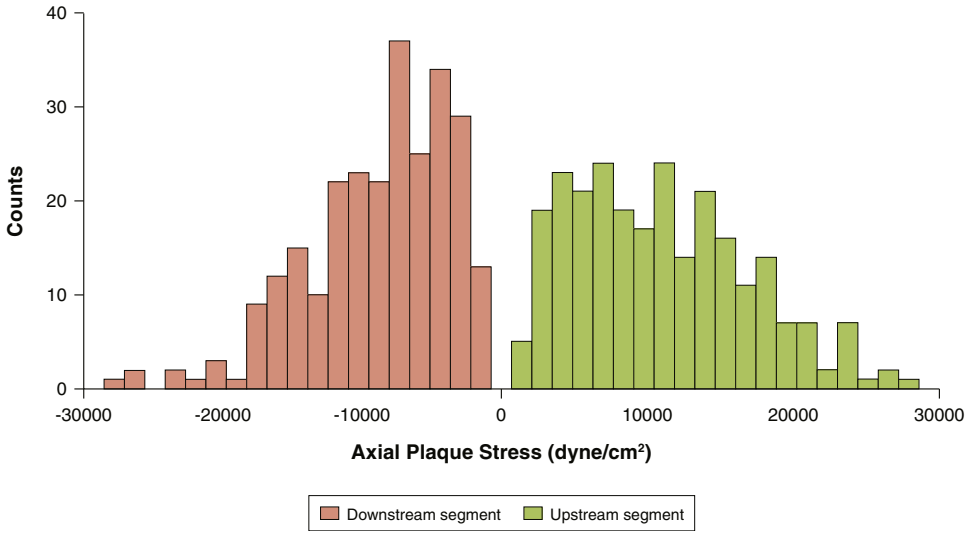

The distribution of the axial plaque stress in the patients' lesions are presented. APS = axial plaque stress.

median interval between coronary CTA and invasive coronary angiography was 29 days (interquartile range: 13 to 49 days), with no clinical events or revascularization between the tests. The distribution of lesions was: left main to left anterior descending coronary artery (n = 72, 64.0%); left circumflex coronary artery (n = 19, 16.7%); right coronary artery (n = 22, 19.3%). The MLA and % area stenosis by coronary CTA were 2.01 ± 0.94 mm^2 and 61.98 ± 13.14%, respectively. The mean values of FFR_{CT} and invasive FFR were 0.78 ± 0.12 and 0.79 ± 0.11 (p = 0.480), respectively (Table 1).

FIGURE 3 Relationship of APS with Pressure Gradient

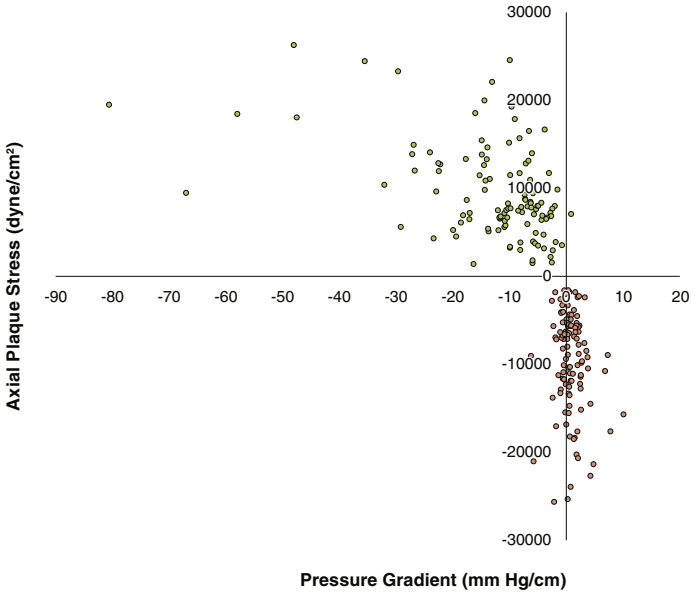

A linear correlation was observed between axial plaque stress and pressure gradient in upstream segments but not in downstream segments due to minimal pressure drop in downstream. APS = axial plaque stress.

APS AND ITS RELATIONSHIP WITH STENOSIS SEVERITY AND LESION LENGTH. The pattern of APS distribution was similar between the data from the patients and from the idealized models (Figure 2, Online Figure 2). Among the total 114 lesions, 81 lesions (71.1%) showed net anterograde axial plaque force with significantly higher axial plaque force in upstream versus downstream segments (5,295.02 ± 3,430.43 dyne vs. 3,318.04 ± 2,298.74 dyne, p < 0.001). Conversely, 33 lesions (28.9%) showed net retrograde axial plaque force with significantly higher downstream axial plaque force, compared with the upstream segment (2,502.25 ± 1,365.57 dyne vs. 3,766.98 ± 374.38 dyne, p < 0.001). In magnitudes, APS ranged up to 30,000 dyne/cm^2, whereas WSS ranged up to 1,000 dyne/cm^2 (Online Figure 3).

The relationship of APS with pressure gradient is presented in Figure 3. In upstream segments, the APS showed a linear relationship with pressure gradient, but not in downstream segments. Although the pressure gradient downstream was minimal, the distribution of downstream APS was highly variable. With

regard to the relationship with lesion severity, the APS linearly increased as the lesion severity increased in upstream segments. However, downstream APS decreased as stenosis severity exceeded a certain degree. When the stenosis severity was greater than an approximately 60% diameter stenosis, the magnitude of downstream APS was reduced (**Figure 4A**). The segmental lesion length also affected the APS. A negative correlation ($r = -0.274$, $p = 0.003$) was observed between the APS and lesion length (**Figure 4B**).

RELATIONSHIP OF APS WITH AXIAL LESION ASYMMETRY. In upstream-dominant lesions ($n = 56$, 49.1%), the average RG for upstream and downstream segments were 0.11 ± 0.05 and 0.06 ± 0.03, respectively ($p < 0.001$). In downstream-dominant lesions ($n = 58$, 50.9%), the average RG for upstream and downstream segments were 0.07 ± 0.03 and 0.12 ± 0.05, respectively ($p < 0.001$) (**Table 2**). In segmental analysis between upstream and downstream segments of stenosis, delta pressure, delta FFR_{CT}, pressure gradient, and WSS were consistently higher in the upstream segment, regardless of the lesion asymmetry (**Table 2**). However, APS exhibited a geometry-dependent distribution. In the upstream-dominant lesions, upstream APS was significantly higher than downstream APS ($11{,}371.96 \pm 5{,}575.14$ dyne/cm^2 vs. $6{,}878.14 \pm 4{,}319.51$ dyne/cm^2, $p < 0.001$). On the other hand, in the downstream-dominant lesions, the downstream APS was significantly higher than upstream APS ($7{,}681.12 \pm 4{,}556.99$ dyne/cm^2 vs. $11{,}990.55 \pm 5{,}556.64$ dyne/cm^2, $p < 0.001$) (**Table 2**). The distribution and differences in hemodynamic parameters according to the plaque geometry showed similar results for a subgroup with more than 40% diameter stenosis (Online Table 1).

Notably, despite no differences in FFR_{CT} (0.83 ± 0.10 vs. 0.80 ± 0.11, $p = 0.121$) or % diameter stenosis ($38.58 \pm 0.11\%$ vs. $39.48 \pm 0.11\%$, $p = 0.661$) between upstream-dominant and downstream-dominant lesions, the APS distinctively showed significant differences according to lesion geometry. WSS did not exhibit a significant difference between the upstream and downstream segments for both groups (upstream WSS: 273.49 ± 181.38 vs. 270.90 ± 124.21, $p = 0.929$; downstream WSS: 147.77 ± 91.84 vs. 153.66 ± 104.89, $p = 0.750$) (**Figure 5**).

Figure 6 illustrates one representative clinical case with an upstream-dominant lesion and depicts the influence of plaque geometry on APS. The coronary CTA image was taken when the patient was asymptomatic as part of a routine health care check-up. In the upstream-dominant lesion at mid-left anterior descending coronary artery, the upstream APS was higher than the stress in the downstream segment.

FIGURE 4 Influence of Lesion Severity and Lesion Length on APS

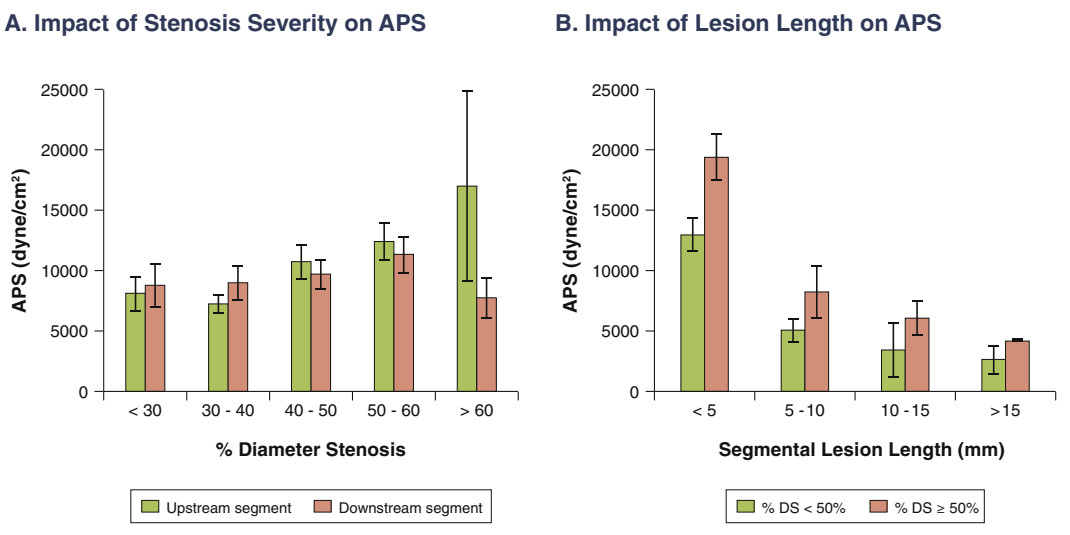

(A) The changes in APS according to the lesion severity (% diameter stenosis) were presented in the patients' lesions. The upstream APS increased as the stenosis severity increased while the downstream APS reached maximum at approximately 60% diameter stenosis and decreased as the lesion severity increased. **(B)** APS was increased as the segmental length decreased. In addition, APS was also higher when the stenosis severity was increased in any given lesion length. APS = axial plaque stress; DS = diameter stenosis.

TABLE 2 Distribution of Hemodynamic Parameters According to the Net Balance of RG of the Lesions in Patients With Coronary Artery Disease

Patients Model (N = 114)	Upstream-Dominant Lesions (n = 56, 49.1%)			Downstream-Dominant Lesions (n = 58, 50.9%)		
	Upstream	Downstream	p Value	Upstream	Downstream	p Value
Radius gradient	0.11 ± 0.05	0.06 ± 0.03	<0.001	0.07 ± 0.03	0.12 ± 0.05	<0.001
Radius gradient, analytic	0.10 ± 0.04	0.06 ± 0.03	<0.001	0.07 ± 0.03	0.12 ± 0.06	<0.001
Δpressure, mm Hg	9.75 ± 8.84	0.18 ± 2.25	<0.001	11.51 ± 8.62	0.69 ± 1.15	<0.001
ΔFFR_{CT}	0.10 ± 0.09	0.002 ± 0.02	<0.001	0.12 ± 0.09	0.01 ± 0.01	<0.001
Pressure gradient, mm Hg/cm^2	14.72 ± 15.48	0.47 ± 1.83	<0.001	11.62 ± 9.26	1.26 ± 2.50	<0.001
WSS, dyne/cm^2	273.49 ± 181.38	147.77 ± 91.84	<0.001	270.90 ± 124.21	153.66 ± 104.89	<0.001
APS, dyne/cm^2	11,371.96 ± 5,575.14	6,878.14 ± 4,319.51	<0.001	7,681.12 ± 4,556.99	11,990.55 ± 5,556.64	<0.001

Values are mean ± SD.

APS = axial plaque stress; FFR_{CT} = coronary computed tomography angiography-derived fractional flow reserve; RG = radius gradient; WSS = wall shear stress.

FIGURE 5 Influence of Lesion Geometry on Hemodynamic Parameters

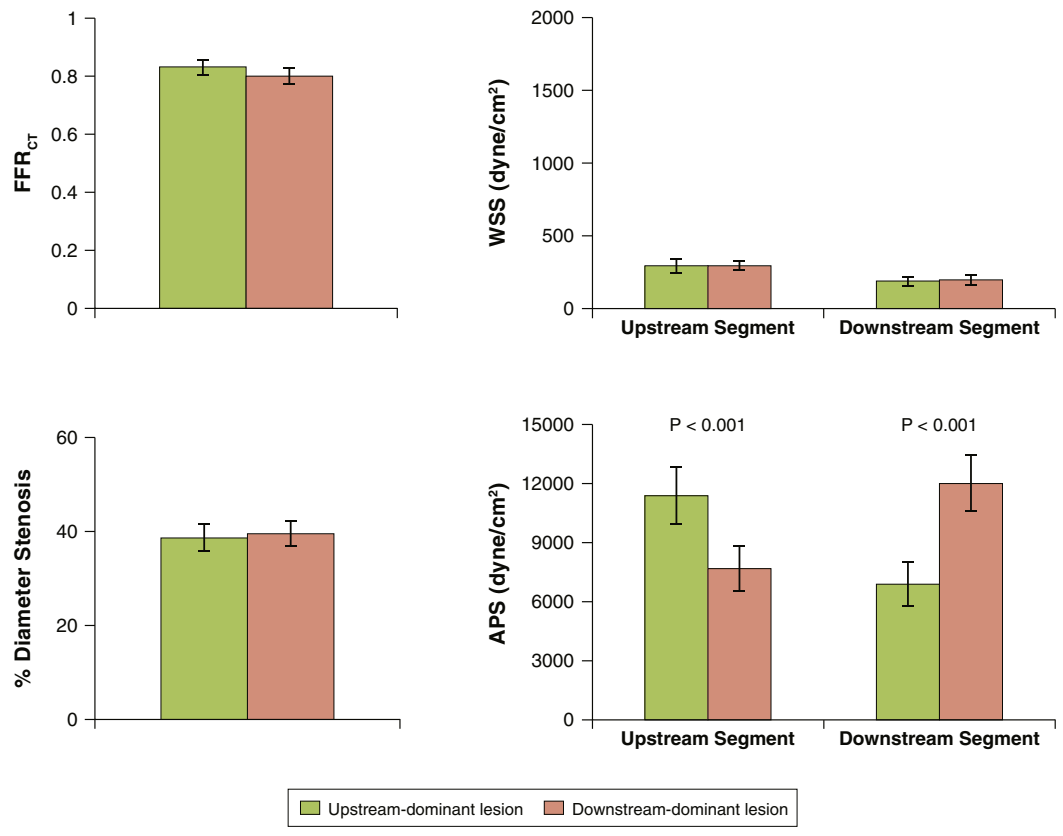

When upstream-dominant and downstream-dominant lesions were compared, there were no significant differences in FFR_{CT} and % diameter stenosis. However, APS exhibited significant changes according to the lesion geometry. In upstream segments, APS of upstream-dominant lesions was significantly higher than that of downstream-dominant lesions. In downstream segments, APS of downstream-dominant lesions were significantly higher than that of upstream-dominant lesions. FFR_{CT} = coronary computed tomography angiography-derived fractional flow reserve; other abbreviations as in Figure 1.

FIGURE 6 Representative Case of Upstream-Dominant Lesion

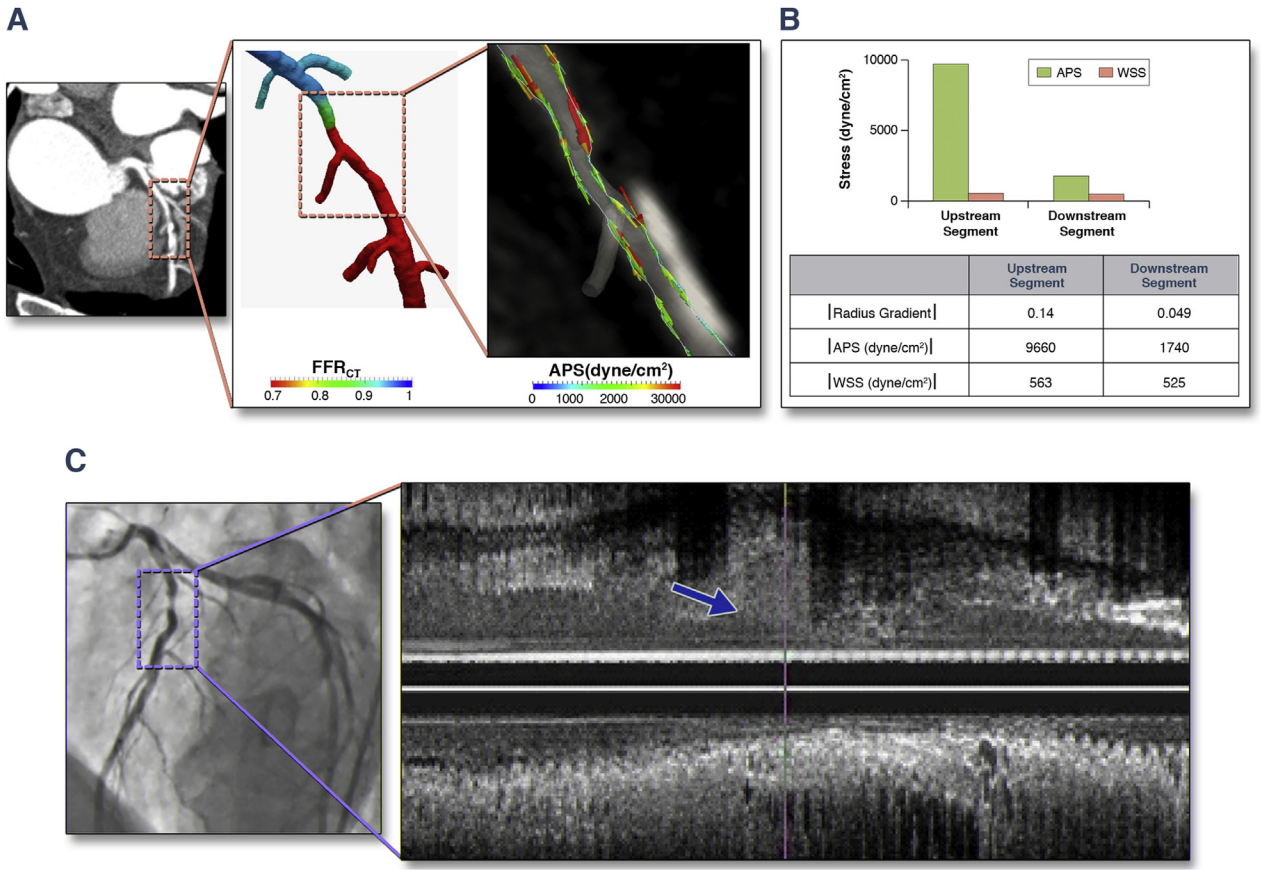

	Upstream Segment	Downstream Segment
|Radius Gradient|	0.14	0.049
|APS (dyne/cm^2)|	9660	1740
|WSS (dyne/cm^2)|	563	525

(A) This patient had undergone coronary computed tomography angiography as part of a routine health care check-up. At that time, the patient did not have any symptoms. **(B)** The coronary computed tomography angiography showed upstream-dominant lesion (upstream RG > downstream RG) in the mid-left anterior descending coronary artery, and the upstream APS was significantly higher than downstream APS. **(C)** About 1 year later, the patient developed acute myocardial infarction, and intravascular ultrasound showed plaque rupture at the same location of highest APS in the upstream segment of the plaque. The **arrow** indicates opening of ruptured cavity. RG = radius gradient; other abbreviations as in Figure 1.

Approximately 1 year later, the patient developed acute myocardial infarction, and the plaque ruptured at the same location of highest APS in the upstream segment.

ASSESSMENT OF LESION ASYMMETRY WITH RG. We compared 2 methods of computing RG in patients' coronary artery lesions in order to determine the practical utility of this metric. Both RGs showed the same trend in both upstream- and downstream-dominant lesions (Table 2). In addition, the relationship of APS with both RGs showed an excellent correlation ($r = -0.956$, $p < 0.001$ for RG, $r = -0.967$, $p < 0.001$ for analytic RG) (Online Figures 4A and 4B). The Pearson correlation coefficient between RG and analytic RG was 0.99 ($p < 0.001$) with the average absolute difference of 0.0036 ± 0.0115 ($p = 0.677$), and interclass correlation was 0.993 ($p < 0.001$) (Online Figure 4C).

DISCUSSION

The assessment of risk for ACS has been one of the most important topics in cardiology for decades (2). However, even among plaques with the same vulnerable features, the hemodynamic forces acting on the plaque can vary and affect the risk of rupture. In an optical coherence tomography study, the thickness of ruptured fibrous cap was thicker in patients with exertion-triggered ACS than those with rest-onset ACS (11). This clinical observation demonstrated the potential role of hemodynamic conditions in the stability of plaques. The present study characterizes the hemodynamic forces acting on plaque and

its relationship with the geometry of stenotic lesions in both patients and idealized models. The similar characteristics of hemodynamic force in relation to lesion geometry observed in idealized stenosis models provided an intuitive and simplified explanation for the results obtained from patient lesions (Online Tables 2 and 3, Online Figures 5 and 6).

ROLE OF HEMODYNAMIC FORCES IN PLAQUE RUPTURE. Previous studies have provided many theoretical and experimental foundations for the mechanisms of plaque progression, transformation, and rupture (1,4,12). Imaging studies have presented several vulnerable plaque features such as thin fibrous cap, microcalcification, large lipid core, active inflammation with macrophage infiltration into the plaque, or well-developed vasa vasorum (2,13). However, these data are related to the composition and organization of the plaque, not mechanical forces. Therefore, adding information on the hemodynamic forces acting on those plaques may provide better risk stratification and treatment strategy.

Among the external hemodynamic forces, WSS has, to date, provided important clues for understanding the mechanisms of the initiation and eventual rupture of atherosclerotic plaque (12). WSS is hypothesized to recruit inflammatory cells and cause vasoconstriction and change in endothelial cell morphology. In this respect, WSS has a particular role in representing the substrate that may contribute to plaque rupture or erosion.

Our study focused on the potential role of APS in plaque rupture and its relationship with lesion geometry. APS could uniquely characterize the stenotic segment and differentiate forces acting on upstream and downstream segments of a plaque. Tanaka et al. (7) reported that the incidence of downstream plaque rupture was up to 36.1% among all rupture cases. Our study found that APS could be higher at the downstream than upstream segment in some lesions. By contrast, WSS and the changes in pressure and FFR were consistently higher in the upstream than in downstream segment.

RELATIONSHIP OF APS WITH LESION CHARACTERISTICS. The relationship of APS with lesion severity showed different characteristics depending upon the sublocations: upstream and downstream segments. Upstream APS linearly increased as lesion severity increased, whereas downstream APS exhibited a concave shape. This result suggests that the risk of downstream rupture can be lower in severe stenosis (>60% to 70% diameter stenosis in our study) as a result of decreased downstream pressure. This phenomenon may explain the reason why Thrombolysis In Myocardial Infarction flow grade 0 was less frequently observed in the downstream rupture cases (7). The significant negative correlation between APS and lesion length in our study provides the explanation for higher incidence of plaque rupture in short and focal lesions than in diffuse ones. When the lesions were divided into upstream-dominant and downstream-dominant lesions, the distribution of APS was significantly different between the 2 groups despite no significant differences in FFR, % diameter stenosis, and WSS pattern in both groups. Therefore, consideration of APS in addition to current plaque evaluation can provide more comprehensive mechanistic explanations for the plaque rupture, including the counterintuitive phenomenon of downstream rupture.

QUANTITATIVE GEOMETRIC INDEX: RG AND ANALYTIC RG. We proposed 2 methods for measuring RG: the first method, denoted as "RG," is a simplified definition based on the radius measurements of 2 discrete locations (starting or ending point, and MLA); the second method, denoted as "analytic RG," is based on the average of radius change over infinitesimal intervals. The 2 definitions of RG showed an excellent correlation with each other and also showed excellent correlations with APS in both idealized and patient-specific models. The 2 methods may be selectively applied according to the complexity of the plaque morphology. If the radius change varies significantly along the length, analytic RG would be more suitable to reflect plaque asymmetry.

POTENTIAL IMPLICATIONS OF APS IN CLINICAL PRACTICE. It is well known that a discrepancy exists between anatomic severity and rupture risk of a plaque (2,14). This discrepancy has provided the impetus for many studies to find high-risk features for plaque rupture in patients with coronary artery disease, with emphasis on plaque morphology and coronary hemodynamics.

In this study, we explored the potential role of APS in plaque rupture. Our study provided 3 major perspectives distinct from previous studies. First, APS uniquely characterized the differences in stress acting on upstream and downstream segments of a plaque in contrast with the WSS and pressure changes, which were consistently higher in the upstream segments. Further, APS revealed the different pattern of force distribution on the upstream and downstream segments according to the severity of stenosis. Second, the dominance of APS varied according to lesion geometry, and this finding can potentially provide an explanation for how plaques can rupture at the downstream segment and why rupture is more frequent in focal lesions than in diffuse ones. Third, APS was different even among

the plaques with the same degree of stenosis and same degree of pressure drop, based on the RG.

Although the current study has focused on characterizing the external hemodynamic forces acting on plaques, it should be remembered that coronary plaque rupture is a complex process that is influenced by diverse factors, including cardiac contractility, aortic blood pressure, pulse pressure, coronary spasm, and endothelial dysfunction. In addition, interpatient variations of microcirculatory resistance originating from structural changes of the myocardium or primary microvascular dysfunction might influence the prediction of the total hemodynamic forces acting on plaque. The role of these diverse potential factors still warrant further investigations in addition to the analysis of hemodynamic forces presented herein.

Considering the complex nature of plaque rupture, the following 3 essential elements should be integrated in order to understand the fundamental mechanism of rupture: composition and organization of plaques, including plaque vulnerability; lesion geometry, including stenosis severity, segmental lesion length, and RG; and external hemodynamic forces, including APS. As noted, plaques can rupture when the stress within the plaque exceeds the strength of the plaque. Although we focused on characterizing the external force acting on the plaque, represented by APS, the external hemodynamic force and lesion geometry would influence the stress within the plaque because the external force and the stress within the plaque should be balanced. Moreover, the lesion geometry, as well as composition and organization of plaques, would determine the strength of plaques. Therefore, patient-specific evaluation of APS and RG will provide additive information in detecting high-risk plaques, and predicting the potential rupture location and subsequent clinical significance of the rupture event for specific plaques.

STUDY LIMITATIONS. Some limitations of this study should be noted. First, although we suggested that APS could provide more reasonable explanations for plaque rupture than other parameters previously reported, we did not present a direct longitudinal causal relationship between the APS and subsequent plaque rupture at the location of high APS. A multicenter clinical study is ongoing to investigate the causal relationship. Second, we focused on the hemodynamic and geometric parameters potentially related to plaque rupture, but did not investigate the material properties of plaques (i.e., plaque vulnerability). Third, the present study did not consider the abrupt change in physiological condition and the impact of mechanical stresses caused by cardiac contraction and relaxation. Further studies using fluid-structure interaction simulation methods incorporating plaque properties and cardiac motion with dynamic changes in heart rate will provide more comprehensive information on the risk of plaque rupture.

CONCLUSIONS

APS uniquely characterizes the stenotic segment and has a strong relationship with lesion geometry. Clinical application of these hemodynamic and geometric indexes may be helpful to assess the future risk of plaque rupture and to determine the treatment strategy for patients with coronary artery disease.

REPRINT REQUESTS AND CORRESPONDENCE: Dr. Bon-Kwon Koo, Department of Internal Medicine and Cardiovascular Center, Seoul National University Hospital, 101 Daehang-ro, Chongno-gu, Seoul 110-744, South Korea. E-mail: bkkoo@snu.ac.kr.

PERSPECTIVES

COMPETENCY IN MEDICAL KNOWLEDGE: Plaque rupture can occur whenever plaque stress exceeds the plaque strength and thus the prediction of plaque rupture may be augmented by accurate assessment of hemodynamic forces. APS characterizes the elevation of hemodynamic stress in both upstream and downstream segments of lesions.

COMPETENCY IN PATIENT CARE AND PROCEDURAL SKILLS: APS characterizes the distribution of plaque stress according to the lesion geometry even for lesions with the same degree of stenosis severity, pressure change, and FFR. A RG, as signified by the luminal radius change over lesion length, allows for comparison of RG upstream-dominant and downstream-dominant lesions; incorporates geometric parameters such as lesion length, minimal lumen area, and stenosis severity. In the present study, we witnessed a strong correlation between APS and RG, which provides supportive evidence of why coronary plaque ruptures may occur in both upstream and downstream segments, and why plaques may rupture in short focal lesions as well as diffuse ones. Patient-specific evaluation of APS and RG provides information in identifying lesions exposed to high hemodynamic forces, which may augment risk stratification of patients with coronary artery disease.

TRANSLATIONAL OUTLOOK: Patients with more focal lesions may have higher APS than those with longer lesions even if the FFR or lesion severity is the same. To confirm the role of APS in plaque rupture, further investigations on the causal relationship between high APS and plaque rupture will be necessary. In addition, consideration of intraplaque stresses will be useful to further characterize the role of APS in the assessment of risk.

REFERENCES

1. Fukumoto Y, Hiro T, Fujii T, et al. Localized elevation of shear stress is related to coronary plaque rupture: a 3-dimensional intravascular ultrasound study with in-vivo color mapping of shear stress distribution. J Am Coll Cardiol 2008;51:645–50.

2. Stone GW, Maehara A, Lansky AJ, et al. A prospective natural-history study of coronary atherosclerosis. N Engl J Med 2011;364:226–35.

3. Li ZY, Howarth SP, Tang T, Gillard JH. How critical is fibrous cap thickness to carotid plaque stability? A flow-plaque interaction model. Stroke 2006;37:1195–9.

4. Li ZY, Gillard JH. Plaque rupture: plaque stress, shear stress, and pressure drop [letter]. J Am Coll Cardiol 2008;52:1106–7; author reply 1107.

5. Dolan JM, Kolega J, Meng H. High wall shear stress and spatial gradients in vascular pathology: a review. Ann Biomed Eng 2013;41:1411–27.

6. Samady H, Eshtehardi P, McDaniel MC, et al. Coronary artery wall shear stress is associated with progression and transformation of atherosclerotic plaque and arterial remodeling in patients with coronary artery disease. Circulation 2011;124:779–88.

7. Tanaka A, Shimada K, Namba M, et al. Relationship between longitudinal morphology of ruptured plaques and TIMI flow grade in acute coronary syndrome: a three-dimensional intravascular ultrasound imaging study. Eur Heart J 2008;29:38–44.

8. Doriot PA. Estimation of the supplementary axial wall stress generated at peak flow by an arterial stenosis. Phys Med Biol 2003;48:127–38.

9. Taylor CA, Fonte TA, Min JK. Computational fluid dynamics applied to cardiac computed tomography for noninvasive quantification of fractional flow reserve: scientific basis. J Am Coll Cardiol 2013;61:2233–41.

10. Taylor AJ, Cerqueira M, Hodgson JM, et al. ACCF/SCCT/ACR/AHA/ASE/ASNC/NASCI/SCAI/SCMR 2010 appropriate use criteria for cardiac computed tomography. A report of the American College of Cardiology Foundation Appropriate Use Criteria Task Force, the Society of Cardiovascular Computed Tomography, the American College of Radiology, the American Heart Association, the American Society of Echocardiography, the American Society of Nuclear Cardiology, the North American Society for Cardiovascular Imaging, the Society for Cardiovascular Angiography and Interventions, and the Society for Cardiovascular Magnetic Resonance. J Am Coll Cardiol 2010;56:1864–94.

11. Tanaka A, Imanishi T, Kitabata H, et al. Morphology of exertion-triggered plaque rupture in patients with acute coronary syndrome: an optical coherence tomography study. Circulation 2008;118:2368–73.

12. Kwak BR, Back M, Bochaton-Piallat ML, et al. Biomechanical factors in atherosclerosis: mechanisms and clinical implications. Eur Heart J 2014;35:3013–20.

13. Otsuka F, Joner M, Prati F, Virmani R, Narula J. Clinical classification of plaque morphology in coronary disease. Nat Rev Cardiol 2014;11:379–89.

14. De Bruyne B, Fearon WF, Pijls NH, et al. Fractional flow reserve-guided PCI for stable coronary artery disease. N Engl J Med 2014;371:1208–17. Erratum in: N Engl J Med. 2014;371:1465.

KEY WORDS axial plaque stress, computational fluid dynamics, coronary artery disease, coronary computed tomography angiography, coronary plaque, pressure, wall shear stress

APPENDIX For an expanded Methods and Results sections as well as supplemental figures and tables, please see the online version of this paper.